ELSEVIER

Biophysical Chemistry 133 (2008) 11 – 18

Biophysical Chemistry

http://www.elsevier.com/locate/biophyschem

Density functional theory study of N–H···O, O–H···O and C–H···O hydrogen-bonding effects on the ^{14}N and ^{2}H nuclear quadrupole coupling tensors of N-acetyl-valine

Mehdi D. Esrafili, Hadi Behzadi, Nasser L. Hadipour *

Department of Chemistry, Tarbiat Modares University, P.O. Box: 14115-175, Tehran, Iran

Received 4 October 2007; received in revised form 11 November 2007; accepted 12 November 2007
Available online 22 November 2007

Abstract

Hydrogen-bonding effects in the crystalline structure of N-acetyl-valine, NAV, were studied using the ^{14}N and ^{2}H quadrupole coupling tensors via density functional theory. The calculations were carried out at the B3LYP level with the 6-311++G(d,p) and 6-311+G(d) basis sets. The theoretical quadrupole coupling components and their relative orientation in the molecular frame axes at the nitrogen site are compared to experimental values. This nucleus is involved in a rather strong intermolecular O═CNH···O═CNH hydrogen bond, $r_{N-H\cdots O(1)} = 2.04$ Å and $\angle N-H\cdots O(1) = 171.53°$. A reasonably good agreement between the experimentally obtained ^{2}H quadrupole coupling tensors and the B3LYP/6–311++G (d,p) calculations is achievable only in molecular model where a complete hydrogen-bonding network is considered.

Keywords: N-acetyl-valine; Electric field gradient; Quadrupole coupling constant; Hydrogen bond; Euler angles

1. Introduction

Among the essential factors determining the native structure of the polypeptides and proteins, hydrogen-bonding interactions play a more important role. They are widely used as indicators of protein secondary structure, i.e. α-helix and β-sheet. Although the accurate characterization of the nature of these interactions in the proteins and polypeptides is a rather formidable task, however, the study of the crystal structure of small peptides and model peptides can be a key to a relatively clear understanding on the protein structure. Numerous studies in various experimental and theoretical fields have been devoted to characterize these hydrogen-bonding interactions in both small peptides and model peptides [1–6].

Because of the electrostatic nature of the hydrogen-bonding interaction, the techniques that deal with the charge distribution around the nuclei seem to be reliable techniques to characterize the nature of hydrogen bonds. Nuclear quadrupole resonance, NQR, spectroscopy is well-established as a versatile technique to study the details of the electronic and nuclear charge distribution around the nucleus of interest [7–10]. Nuclei with spin angular momentum, *I*, greater than one-half, $I > 1/2$, have nuclear electric moment, *eQ*, which interacts with electric field gradient, EFG, originated at the site of quadrupole nuclei [11]. EFG is a tensor quantity and is, therefore, capable of providing six pieces of information, namely, the magnitude and direction of the three principal components. The nuclear quadrupole coupling constant, QCC, and its associated asymmetry parameter, η_Q, are those experimentally measurable NQR parameters of which the former indicates the amount of interaction of *eQ* with the EFG tensor and the latter measures the symmetry of the EFG tensor. Since the magnitude and orientation of the quadrupole coupling tensor are fundamentally related to the local environment around the nuclei, quadrupole coupling tensor seems to be a useful tool to gain insight into the conformation and native structure of the backbone of polypeptides. Recently, extensive experimental and theoretical ^{2}H, ^{14}N and ^{17}O NQR studies on the polypeptides have shown that there is a direct relationship between the molecular structure and NQR parameters. For example, Torrent et al. indicated that QCC is a useful parameter for the characterization of small protein fragment at two secondary structures, i. e. α-helices and

---

* Corresponding author. Tel.: +98 2188011001 3495; fax: +98 218800 9730.
E-mail address: hadipour@modares.ac.ir (N.L. Hadipour).

0301-4622/$ - see front matter © 2007 Elsevier B.V. All rights reserved.
doi:10.1016/j.bpc.2007.11.006

β-sheets [12]. Based on the solid state NMR study of the model peptide N-acetyl valine, Haeberlen et al. reported a close relationship between the strength of the OCNH···O═CNH and O═COH···HNCO hydrogen bonds and the magnitude of the ^{2}H quadrupole coupling constants and asymmetry parameters [13].

N-acetyl valine, NAV, is a valine derivative in which, an acetyl group is substituted for amine hydrogen; see Fig. 1. NAV has been chosen to be studied in the present work for several reasons. First, the hydrogen-bonding interaction site of the amide hydrogen with its neighboring molecules is similar to the peptides, which makes NAV as an important model peptide for investigation the properties of peptide bond in proteins and polypeptides. Second, the crystalline structure of NAV has been accurately determined by X-ray crystallography at 293 K [14]. Third, crystalline NAV exhibits an unusual C–H···O hydrogen-bonding interaction, and therefore, can be a simple model to investigate the influence of this hydrogen bond on the hydrogen EFGs in peptides. Fourth, in spite of the fact that several theoretical and experimental efforts have been reported to the strong dependency of the chemical shift values on the hydrogen-bonding interactions of NAV [13,15,16], there is still a lack of quantitative investigation of intermolecular hydrogen-bonding effects on the ^{14}N and ^{2}H quadrupole coupling tensors in the crystalline NAV.

It is well-known that quantum chemistry calculations can provide an independent source of EFG tensors and their relative orientations in the molecular frame. Although the experimental approaches are more suitable for obtaining

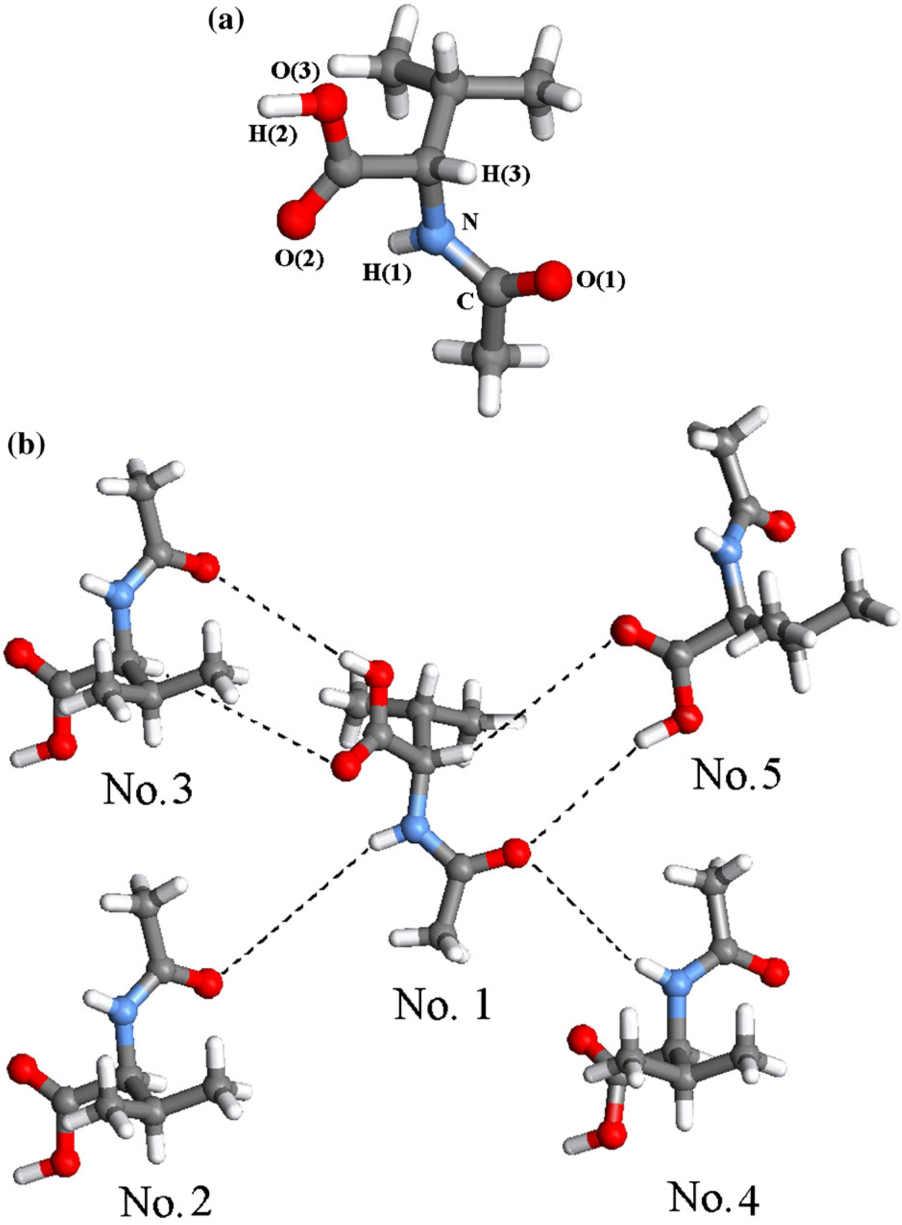

Fig. 1. a) Monomer and b) Illustration of intermolecular hydrogen bonds in the crystalline NAV.

information about the nature of hydrogen bonds, however, the theoretical calculations can be confidently used as a complementary tool to interpret the experimentally measured NQR parameters. In a series of previous studies, it has been theoretically demonstrated that the intermolecular hydrogen-bonding interactions have a major influence on the ^{14}N and ^{2}H quadrupole coupling tensors of the small peptides and model peptides [17–22]. Although the sensitivity of the eigenvalues of the ^{14}N and ^{2}H quadrupole coupling tensors to such interactions has been extensively established, a quantitative study of how the tensor eigenvectors and their relative orientation to the molecular frame axes vary, due to the hydrogen bond interactions, to our knowledge, is so far absent from the literature. The main objective of the present study is to systematically investigate the influence of intermolecular hydrogen bonds on both magnitude and orientation of ^{14}N and ^{2}H in the crystalline NAV. We hopefully expect that these results will expand upon the existing research into the more general context of structural determination, and as an initial stage for understanding the variation of the magnitude and orientation of the ^{14}N and ^{2}H quadrupole coupling tensors in biologically interesting peptides and proteins.

2. Definition and methods

^{14}N and ^{2}H EFG tensors were calculated using the GAUSSIAN 98 suite of programs [23]. Among the various functionals for DFT calculation, Becke three parameter hybrid functional combined with Lee-Yang-Parr correlation functional designated B3LYP, with the 6-311++G(d,p) and 6-311+G(d) standard basis sets were used [24]. Various combinations of diffuse and polarization functions are incorporated in these two basis sets that are necessary for computation of the EFG tensors of hydrogen and nitrogen atoms involved in the hydrogen bond. Our previous experiences reveal that the 6-311++G(d,p) and 6-311+G(d) basis sets usually lead to satisfactory EFG values [25–27]. The calculated principal EFG values, q_{ii}, were used to obtain the nuclear quadrupole coupling components from the equation:

$$\chi_{\mathrm{ii}}(\mathrm{MHz}) = e^2\mathrm{Q}\mathrm{q}_{\mathrm{ii}}/h, \quad i = x, y, z \tag{1}$$

where eQ is the nuclear quadrupole moment of the ^{14}N and ^{2}H (in fm^2). The NQR parameters are often reported experimentally as the nuclear quadrupole coupling constant and asymmetry parameter defined as [28]:

$$\mathrm{QCC}(\mathrm{MHz}) = e^2\mathrm{Q}\mathrm{q}_{\mathrm{zz}}/h$$

$$\eta_Q = \left|\frac{q_{\mathrm{yy}} - q_{\mathrm{xx}}}{q_{\mathrm{zz}}}\right|, \quad 0 \leq \eta_Q \leq 1. \tag{2}$$

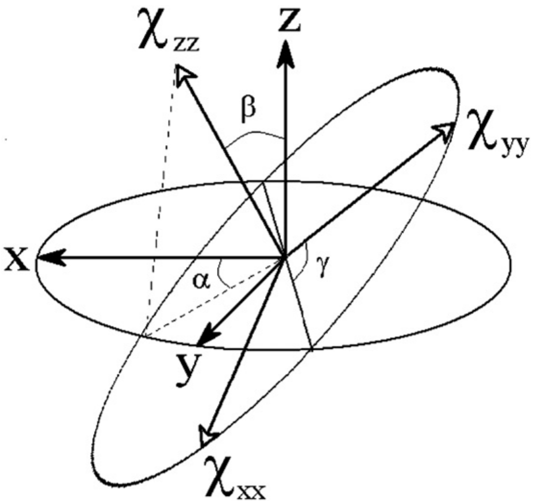

Fig. 2. Orientation of the principal components of the ^{14}N and ^{2}H EFG tensors relative to the molecular frame axes. α, β and γ are Euler angles relating the EFG tensors and molecular frame axes.

In addition to the principal components, EFG tensor can be described with three Euler angles as demonstrated in Fig. 2. It is straightforward to obtain a rotation matrix, $\hat{R}$ which describes how to rotate an axes frame (x, y, z) fixed on an object within a frame (X, Y, Z). The rotation matrix relating principal axes system, PAS, of EFG tensor to the molecular axes system follows from [28]:

$$\hat{R}(\alpha,\beta,\gamma) = \hat{R}_z(\gamma)\hat{R}_y(\beta)\hat{R}_z(\alpha) \tag{3}$$

$$\hat{R}(\alpha,\beta,\gamma)\begin{bmatrix} x \\ y \\ z \end{bmatrix} = \begin{bmatrix} \cos(\alpha)\cos(\beta)\cos(\gamma) - \sin(\gamma)\cos(\alpha) & \cos(\alpha)\cos(\beta)\sin(\gamma) + \sin(\gamma)\cos(\alpha) & -\cos(\gamma)\sin(\beta) \\ \cos(\alpha)\cos(\beta)\cos(\gamma) - \sin(\gamma)\cos(\alpha) & \sin(\gamma)\cos(\beta)\cos(\alpha) + \cos(\gamma)\cos(\alpha) & \sin(\gamma)\sin(\beta) \\ \sin(\beta)\cos(\alpha) & \sin(\beta)\cos(\alpha) & \cos(\beta) \end{bmatrix}\begin{bmatrix} x \\ y \\ z \end{bmatrix}$$

in which $\hat{R}_z(\alpha)$, for example, describes the rotation of PAS by α around the z axis.

The accurate calculation of magnitude and orientation of the principal components of quadrupole coupling tensor requires the positions of all atoms to be determined with high precision. As it is known, X-ray crystallography fails to characterize the accurate positions of those atoms do not scatter X-rays effectively. Therefore, the positions of hydrogen atoms are not known with certainty even for highly resolved crystal structures. The resulted errors in the bond distances and angles of hydrogen atoms due to this uncertainty has been shown to have a significant effect on the calculated quadrupole coupling tensors [15,27,29–31]. Therefore, hydrogen atom positions were optimized at the B3LYP/6-311G level of theory for both monomer and pentamer cluster. This level of theory has been previously shown to give hydrogen atom position comparable to neutron diffraction values for a variety of systems [16,32–34].

3. Results and discussion

In the present study, we calculated the ^{14}N and ^{2}H EFG tensors of NAV in its crystalline structure to investigate the influence of intermolecular hydrogen-bonding interactions. To achieve the aim, the calculations were performed for two molecular models including an isolated gas phase (monomer) and a pentamer cluster; see Fig. 1 and Table 1 for details. Tables 2–5 represent the calculated ^{14}N and ^{2}H quadrupole coupling tensors and related Euler angles for the monomer and

Table 1
Structure parameters of NAV in its crystalline structure at 293 K

Geometrical parameters	Donor-acceptor	Distances and angles [a]
$r_{\mathrm{N\cdots O}\ (1)}$	Central-number 2 $(2-x, -.5+y, 1.5-z)$	3.03 Å
$r_{\mathrm{O\cdots O}\ (1)}$	Central-number 3 $(1-x, -.5+y, 1.5-z)$	2.72 Å
$r_{\mathrm{C\cdots O}\ (2)}$	Central-number 5 $(1-x, .5+y, 1.5-z$	3.46 Å
$r_{\mathrm{H1\cdots O}\ (1)}$	Central-number 2 $(2-x, -.5+y, 1.5-z)$	2.04 Å
$r_{\mathrm{H2\cdots}\ (1)}$	Central-number 3 $(1-x, -.5+y, 1.5-z)$	1.73 Å
$r_{\mathrm{H(3)\ \cdots O}\ (2)}$	Central-number 5 $(1-x, .5+y, 1.5-z)$	2.47 Å
∠N–H···O (1)	Central-number 2 $(2-x, -.5+y, 1.5-z)$	171.53°
∠O–H···O (1)	Central-number 3 $(1-x, -.5+y, 1.5-z)$	175.55°
∠C–H···O (2)	Central-number 5 $(1-x, .5+y, 1.5-z)$	165.64°

[a] Hydrogen atom positions were optimized at the B3LYP/6-311G level of theory.

Table 3
Calculated Euler angles (in deg) for nitrogen atom in the monomer and target molecule in the cluster

Nucleus	Basis set	Monomer			Cluster		
		α	β	γ	α	β	γ
N	6-311++G(d,p)	61.72	38.66	33.49	66.91	64.44	87.19
	6-311+G(d)	60.75	38.30	33.62	65.66	64.90	87.93

the target molecule in the pentamer cluster of crystalline NAV. In the following section, we will discuss the B3LYP/6-311++G(d,p) results for the ^{14}N and ^{2}H EFG tensors, separately.

3.1. Nitrogen EFG tensors

In this section, the influence of the hydrogen-bonding interactions on the quadrupole coupling tensors at the site of ^{14}N nucleus of the monomer (as a baseline for the ^{14}N NQR tensors) and the target molecule in the pentamer cluster are discussed; see Tables 2 and 3. The quadrupole coupling components, χ_{ii}, were obtained from the calculated principal components of EFG tensors using the recently reported value for the ^{14}N electric quadrupole moment of $eQ(^{14}\mathrm{N})=20.44$ fm^2 [35]; see Eq. (1).

As mentioned earlier, the presence of peptide type hydrogen bond in crystalline NAV provides one with the chance to examine the influence of this interaction on the ^{14}N quadrupole coupling tensor and its orientation in the molecular frame axes. As Fig. 1 indicates, the hydrogen bond at the amide site of the target molecule involves oxygen atom of the same group of neighboring molecule (molecule number 2). X-ray crystallography studies reveal that NAV molecules make a layer like structure in the crystalline phase [14,36]. A quick look at the entire unit cell, shows that O═CNH···HNC═O type hydrogen bond joins the molecules in two neighboring anti-parallel layers. Our earlier study on α-glycylglycine suggested the significance of including this hydrogen-bonding interaction in determining the ^{14}N quadrupole coupling tensors [21].

As the results of Table 2 illustrate, due to the hydrogen bonding interactions, all principal ^{14}N quadrupole coupling components deviate significantly from the monomer values. More specifically, from the monomer to the target molecule in the cluster, hydrogen-bonding interactions cause a 0.86 MHz reduction in QCC(^{14}N) parameter. It is also interesting to see that the η_Q (^{14}N) is improved 17 units depending on whether the NAV molecule is in the monomer or in the hydrogen-bonded network. It should be noted that these changes are much larger than those seen for our previous studied crystalline α-glycylglycine (ca. Δ(QCC(^{14}N)) = 0.164 MHz for one N–H···O hydrogen bond) [21]. Comparison of the structure parameters of these two compounds in their crystalline phases, reveal that unlike hydrogen bond length, there is a significant difference in the hydrogen bond angle, ∠N–H···O, from NAV to α-glycylglycine. The basic structural parameters for the amide fragment of α-glycylglycine are obtained to be $r_{\mathrm{N-H\cdots O}}=1.99$ Å and ∠N–H···O = 157.84° [37], while the corresponding values for NAV molecule in the solid state are $r_{\mathrm{N-H\cdots O}}=2.04$ Å and ∠N–H···O = 171.53° [14]. Therefore it is concluded that the contribution of hydrogen bond angle has made NAV amide site more sensitive than α-glycylglycine to feel the neighboring effects. However, comparison of the calculated ^{14}N quadrupole coupling components and asymmetry parameters of NAV with the available experimental data shows that there is a good agreement between the theoretical and experimental parameters [38]; see Table 2. Particularly, η_Q is in excellent agreement with the experimental data, indicating that small errors in the calculated magnitude of principal elements tend to cancel out together. These features also illustrate that the CO^{14}NH site of the target molecule in the NAV hydrogen-bonded network approximately feels the same chemical

Table 2
Calculated quadrupole coupling components (in MHz) and asymmetry parameters of ^{14}N

Model	Basis set	χ_{xx}	χ_{yy}	χ_{zz}	η_Q
Monomer	6-311++G(d,p)	1.87	2.53	4.41	0.15
	6-311+G(d)	1.92	2.57	4.49	0.14
Pentamer cluster	6-311++G(d,p)	1.22	2.33	3.55	0.32
	6-311+G(d)	1.30	2.31	3.61	0.28
Experimental [a]		1.09	2.12	3.21	0.32

[a] Experimental values from Ref. [38].

Table 4
Calculated quadrupole coupling components (in kHz) and asymmetry parameters of ^{2}H nuclei

Model	Nucleus	Basis set	χ_{xx}	χ_{yy}	χ_{zz}	η_Q
Monomer	H (1)	6-311++G(d,p)	89.33	144.95	234.29	0.24
		6-311+G(d)	86.00	136.86	222.86	0.23
	H (2)	6-311++G(d,p)	92.47	115.12	207.59	0.11
		6-311+G(d)	88.65	108.35	197.00	0.10
	H (3)	6-311++G(d,p)	150.68	157.03	307.62	0.02
		6-311+G(d)	147.07	153.06	300.13	0.02
Pentamer cluster	H (1)	6-311++G(d,p)	78.91	132.88	211.80	0.25
		6-311+G(d)	75.69	125.86	201.54	0.25
	H (2)	6-311++G(d,p)	73.96	93.87	167.84	0.12
		6-311+G(d)	72.29	90.14	162.43	0.11
	H (3)	6-311++G(d,p)	146.0	153.74	299.74	0.03
		6-311+G(d)	142.68	149.96	292.64	0.03
Experimental [a]	H (1)		88.33	124.26	212.60	0.17
	H (2)		72.00	88.00	160.00	0.10

[a] Experimental values from Ref. [13].

Table 5
Calculated Euler angles (in deg) for hydrogen atoms in the monomer and target molecule in the cluster

Nucleus	Basis set	Monomer			Cluster		
		α	β	γ	α	β	γ
H (1)	6-311++G(d,p)	51.76	45.43	46.13	73.73	12.69	73.17
	6-311+G(d)	51.72	46.35	46.38	73.65	13.66	72.72
H (2)	6-311++G(d,p)	19.02	14.27	34.65	40.60	10.00	68.34
	6-311+G(d)	18.05	13.56	34.72	39.17	10.05	67.25
H (3)	6-311++G(d,p)	19.45	26.55	55.56	30.32	62.37	32.22
	6-311+G(d)	19.72	26.56	55.86	30.44	61.48	32.94

environment as in the actual solid phase. Moreover, the experimental solid state NMR study was done at 298 K. Therefore a portion of disagreements between the calculated and experimental data is believed to be due to the temperature difference.

As shown in Fig. 3 and Table 3, ^{14}N quadrupole coupling tensor orientation shows some degree of sensitivity upon the OCNH···O═CNH hydrogen-bonding environment. To the best of our knowledge, it is the first time that χ_{ii} orientation of ^{14}N nucleus involved in the peptide bond has been examined. As also can be seen from Table 3, hydrogen bond interaction was found to have different influences on the calculated Euler angles of the amide ^{14}N nucleus. While α component increases from the monomer to the target molecule in the cluster by 5.2°, the changes for both β and γ angles are noticeable; $\Delta\beta$=25.8° and $\Delta\gamma$=53.7°. These features suggest that in agreement with the magnitude of principal components, including the hydrogen-bonding interactions has a great influence on the orientation of ^{14}N quadrupole coupling components. Similar dependency has been reported in a previous theoretical work for ^{15}N NMR orientation of NAV on the hydrogen-bonding interactions [16].

The accuracy of the angle defining the ^{14}N quadrupole coupling tensor obtained by our theoretical methods can be estimated by comparing calculated results with experimental available data. Recently, based on the ^{14}N single crystal NMR study, Stark et al. indicated that ^{14}N quadrupole tensor orientation in crystalline NAV is in a manner that the χ_{xx} component approximately lies in the N–H bond vector. On the basis of the molecular symmetry, they also expected that one of the other two principal components to lies approximately perpendicular to the C–N–C plane and the third to be orthogonal to these two orientations [38]. However, angles calculated using the whole NAV cluster have been obtained in a such a way that χ_{xx} and χ_{yy} make a 13.2° and 103.2° with the N–H bond direction, respectively. We also found an excellent agreement between the theoretical and experimental orientation of χ_{zz} component which, as shown in Fig. 3, is indicated lies perpendicular to the N–H bond. The remaining small discrepancies between the calculated and experimental tensor orientations can be attributed to one or more possible factors: differences between the structure used in our calculations and experimental study; intrinsic limitations in the ^{14}N EFG calculations or other neglected intermolecular interactions within the used molecular cluster.

3.2. Hydrogen EFG tensors

As shown in the previous part, hydrogen-bonding interactions affect remarkably the ^{14}N quadrupole coupling components and their orientations in the NAV molecular frame. In this part, we will discuss the influence of hydrogen-bonding interactions on the calculated ^{2}H quadrupole coupling components and their relative orientation in the NAV molecular frame axes. The recently reported standard $eQ(^{2}H)$=2.86 fm^{2} value [35] was used for calculation of the quadrupole coupling components; see Table 4.

As seen from Fig. 1, the target molecule in the cluster is capable of participate in a variety of intermolecular OCN-H···O═CNH, O═COH···OCNH and CH···O═COH hydrogen bond interactions with the molecules number 2–5. The main concern of this study at this part is to elucidate the hydrogen-bonding effect on the quadrupole coupling tensors, specifically those contributing in the peptide type hydrogen bond. As the results of Table 4 illustrate, the calculated χ_{ii} (^{2}H) values at the amide site exhibit a rather strong dependency on the hydrogen-bonding interactions. This is consistent with the general observation that the hydrogen-bonding interactions tend to reduce the QCC(^{2}H) values [39]. There is, however, a significant reduction for ^{2}H(1) QCC value, ΔQCC(^{2}H)=22.49 kHz. The calculated QCC(^{2}H) and η_Q values for H(1) of the target molecule have been obtained to be 211.80 kHz and 0.25, respectively. These values, which are obtained by taking the whole cluster into consideration, is expected to be close to the corresponding experimental values [13], QCC(^{2}H)=212.60 kHz and η_Q(^{2}H)=0.17, respectively. A similar observation has been reported in our previous study on the ^{2}H quadrupole tensor of α-glycylglycine [21].

It has been found from Table 4 that η_Q(^{2}H) value at the amide hydrogen site does not show necessarily any dependency on the hydrogen-bonding interactions. In assessing the significance of η_Q(^{2}H) values, one must keep in mind that electronic contribution to the EFG at hydrogen sites arises almost entirely from centers other than the hydrogen, since spherical electronic cloud around these nuclei has no contribution. As the OCNH···O═CNH hydrogen bond sets in, the

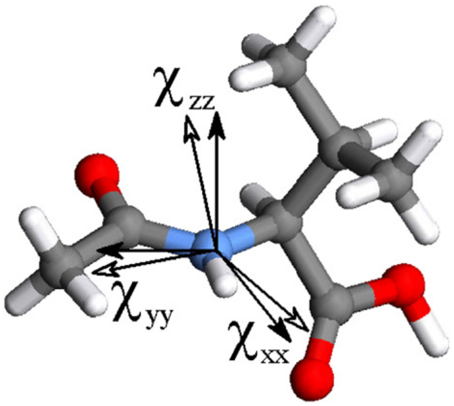

Fig. 3. Orientation of the ^{14}N quadrupole coupling components, χ_{ii}, of NAV (empty and solid arrows refer to the monomer and target molecule in the cluster, respectively).

electron distribution around the hydrogen nucleus is polarized in the direction of oxygen atom and makes a significant reduction in the magnitude of all three individual EFG components. However, in η_Q, the three diagonal components of the EFG are involved in its definition. From the data shown in Table 4, it is clear that the observed non dependency for $\eta_Q(^2H)$ value arises from the fact that as the hydrogen atom interacts with its neighbor, the q_{ii} values change in a similar direction and therefore remains invariable the symmetry of the ^2H EFG tensor. This observation is completely consistent with the early ^2H NQR studies [26,40,41].

In comparison with the amide site, the hydrogen atom at the carboxylic group contributes in a shorter hydrogen bond, $r_{O–H\cdots O}=1.73$ Å and $\angle O–H\cdots O=175.55°$. It interacts with the O (1) atom of molecule number 3 that is located in the neighboring anti-parallel layer. Calculated results from both computational levels reveal that due to the hydrogen bonding interactions, QCC(^2H) at the carboxylic site decreases approximately by 40 kHz. On the other hand, both smallest and intermediate components of quadrupole coupling tensor, χ_{xx} and χ_{yy}, show approximately a reduction of 20 kHz from the monomer to the target molecule in the cluster. These changes are also reflected in the asymmetry parameter, η_Q. For example, η_Q value of ^2H (2) is found to remain practically unchanged from the monomer to the cluster. Meanwhile, the calculated ^2H (2) quadrupole coupling tensor meet the related experimentally reported data [13].

In simulating the actual hydrogen-bonded network of crystalline NAV, molecule number 5 was taken into consideration. This molecule is located at the same layer of the molecule number 2 and is capable of making a weak CH···O hydrogen bond with the target molecule, $r_{C–H\cdots O}=2.47$ Å, $\angle C–H\cdots O=165.64°$. Because of the unusual nature of CH···O hydrogen-bonding in the biological systems, it is, therefore, of interest to examine the effect of this interaction on the ^2H in more detail. However, as the results of Table 4 illustrate, including the CH···O type hydrogen-bonding interaction does not change the asymmetry parameters, but it decreases the calculated QCC(^2H) value approximately by 8 kHz. This is due to the limited involvement of this group in the intermolecular interaction of NAV in its solid phase.

Since the interaction of the EFG and nuclear quadrupole moment is essentially a local phenomenon, orientation of ^2H quadrupole coupling components is known to be intimately related to the local environment around the ^2H nuclei, therefore, making the ^2H quadrupole coupling tensor orientation as a useful tool to gain better insights into conformation of the backbone of peptides and proteins [13,42]. Fig. 4 represents the obtained relative orientation of ^2H quadrupole coupling components in the molecular frame axes. As also indicated in Table 5, including hydrogen-bonding interactions has remarkable influences on all ^2H Euler angles. It is obvious from Fig. 4 that at the amide hydrogen site, the greatest quadrupole coupling component orientates in the N-H bond direction. The angle deviation from the N–H bond direction is calculated to be approximately 1.4° However, single crystal deuterium NMR study indicated that in crystalline NAV, χ_{zz} deviates only 1.8° from the N–H direction [13]. Furthermore, both smallest and intermediate components were found to be perpendicular to the N–H bond direction. At the site of carboxylic hydrogen atom, however, the orientation of quadrupole coupling components are slightly different. For this nucleus, χ_{zz} tends to lie in the O–H direction from the monomer to the target molecule in the cluster. This is in excellent consistent with the previous experimental studies of orientation of deuterium quadrupole coupling tensors in NAV and comparable compounds [13,43]. For hydrogen atom contributed in C–H···O hydrogen bond, χ_{zz} deviates approximately by 46.0° from the C–H bond direction. Moreover, orientation of both χ_{xx} and χ_{yy} components deviate remarkably from the monomer to the cluster; see Fig. 4.

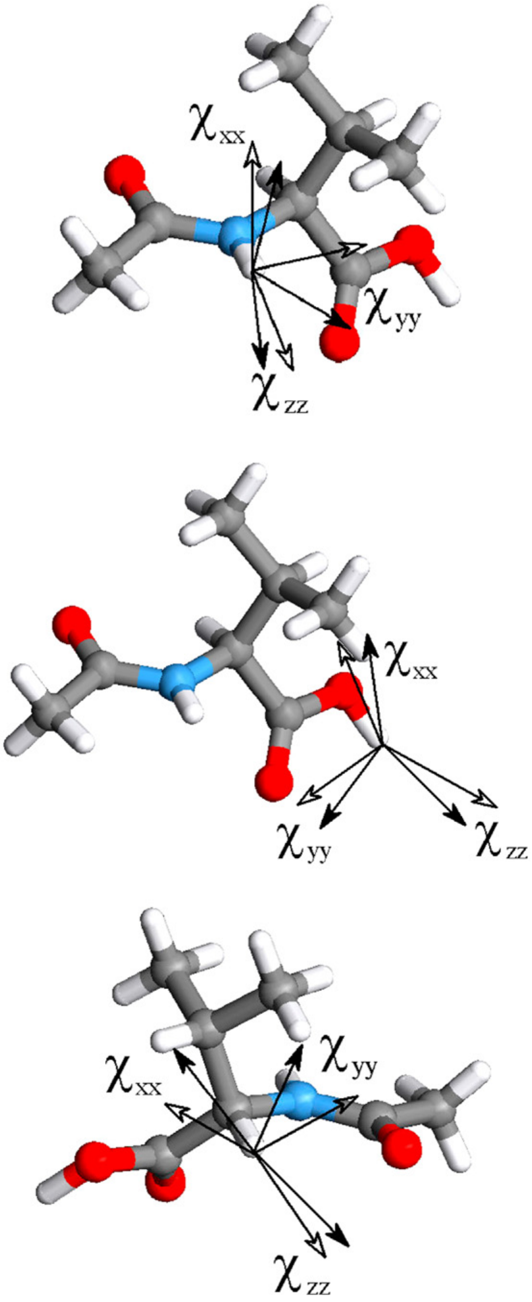

Fig. 4. Orientation of the ^2H quadrupole coupling components, χ_{ii}, of NAV (empty and solid arrows refer to the monomer and target molecule in the cluster, respectively).

To the best of our knowledge, there is neither experimental nor theoretical ^{2}H quadrupole coupling tensor orientation for CH···O hydrogen bond in the literature.

Finally, the results from the 6-311++G (d,p) and 6-311+G (d) basis sets were compared. As can be shown in Tables 2 and 4, it is found that calculated χ_{ii} values show a rather dependency on the basis set size. On the other hand, the orientations of ^{14}N and ^{2}H quadrupole coupling tensors in the molecular frame of reference show a striking insensitivity to the size of the basis sets as compared to the principal components; see Tables 3 and 5. In agreement with the previous studies, both diffusion and polarization functions seem to be essential for accurately reproducing the experimental principal values of the EFG tensors. Furthermore, the application of larger basis sets does not appear to systematically improve the quadrupole coupling tensor orientations. Therefore, this property of quadrupole coupling tensor makes the study of ^{14}N and ^{2}H χ_{ii} tensor orientation possible in large biologically systems.

4. Concluding remarks

On the basis of the results obtained in this investigation, it is concluded that EFG tensors of nitrogen and hydrogen atoms in the hydrogen-bonding interactions are appropriate parameters to characterize the property of these interactions. The comparison of the calculated quadrupole coupling tensors of nitrogen and hydrogen nuclei in the monomer and the target molecule in a pentameric cluster reveal the influence of O═COH···OCNH, OCNH···O═CNH and CH···O═COH type hydrogen bonds on the EFG tensors and related orientations at the site of ^{14}N and ^{2}H nuclei in crystalline NAV. Using the B3LYP functional with the 6-311++G (d,p) and 6-311+G (d) basis sets, calculations can reproduce reasonably the experimental reported values. The presence of O═CNH···OCNH hydrogen bond for amide nitrogen causes a decrease of 0.86 MHz in the QCC(^{14}N) and an increase of 17 units in the η_Q(^{14}N) values. However, the QCC(^{14}N) and η_Q(^{14}N) values at the amide site were determined to be 3.55 MHz and 0.32, respectively, which are in reasonable agreement with the available experimental values (QCC = 3.21 MHz, and $\eta_Q = 0.32$). The computed relative orientation of ^{14}N eigenvectors also meets the experimental values. The hydrogen-bonding effects on the calculated ^{2}H quadrupole coupling tensor at the amide and carboxylic sites are also noticeable. For these nuclei, Δ(QCC) = 22.49 and 40 kHz reveal the major role of amide and carboxylic groups in contributing to the intermolecular hydrogen-bonding interactions in the crystalline NAV, respectively. Moreover, our obtained results indicated that for the ^{2}H nucleus involved in the CH···O═COH hydrogen bond interaction, χ_{zz} component deviates approximately by 46.0° from the C–H bond direction and orientation of both χ_{xx} and χ_{yy} components deviate remarkably from the monomer to the cluster.

References

[1] R.E. Stark, L.E. Jelinski, D.J. Ruben, D.A. Torchia, R.G. Griffin, ^{13}C chemical shift and ^{13}C–^{15}N dipolar tensors for the peptide bond: [1–^{13}C] glycyl[^{15}N]glycine·HCl·H$_2$O, J. Magn. Reson. 55 (1983) 266–273.

[2] H. Le, E. Oldfield, Ab initio studies of amide-N-15 chemical shifts in dipeptides: applications to protein NMR spectroscopy, J. Phys. Chem. (1996) 16423–16428.

[3] J. Birn, A. Poon, Y. Mao, A. Ramamoorthy, Ab initio study of C-13 alpha chemical shift anisotropy tensors in peptides, J. Am. Chem. Soc. 126 (2004) 8529–8534.

[4] C. Scheurer, N.R. Skrynnikov, S.F. Lienin, S.K. Straus, R. Brüschweier, R.R. Ernst, Effects of dynamics and environment on N-15 chemical shielding anisotropy in proteins. A combination of density functional theory, molecular dynamics simulation, and NMR relaxation, J. Am. Chem. Soc. 121 (1999) 4242–4251.

[5] Q. Teng, M. Iqbal, T.A. Cross, Determination of the carbon-13 chemical shift and nitrogen-14 electric field gradient tensor orientations with respect to the molecular frame in a polypeptide, J. Am. Chem. Soc. 114 (1992) 5312–5321.

[6] K.W. Waddell, E.Y. Chekmenev, R.J. Wittebort, Single-crystal studies of peptide prolyl and glycyl N-15 shielding tensors, J. Am. Chem. Soc. 127 (2005) 9030–9035.

[7] B. Nogaj, Hydrogen-bond theories and models based on nuclear quadrupole resonance spectroscopy studies, J. Phys. Chem. 91 (1987) 5863–5869.

[8] M.J. Hunt, A.L. Mackay, Deuterium and nitrogen pure quadrupole resonance in amino acids. II, J. Magn. Reson. 22 (1976) 295–301.

[9] M.J. Hunt, A.L. Mackay, Deuterium and nitrogen pure quadrupole resonance in deuterated amino acids, J. Magn. Reson. 15 (1974) 402–414.

[10] J. Murgich, Y. Aray, H.J. Soscum, N-14 NQR and ab initio MO calculations of quinolines, naphthyriden, and benzodiazines, J. Phys. Chem. 96 (1992) 9198–9200.

[11] R. Bersohn, Nuclear electric quadrupole spectra in solids, J. Chem. Phys. 20 (1952) 1505–1509.

[12] M. Torrent, D. Mansour, E.P. Day, K. Morokuma, Quantum chemical study on oxygen-17 and nitrogen-14 nuclear quadrupole coupling parameters of peptide bonds in α-helix and β-sheet proteins, J. Phys. Chem. A 105 (2001) 4546–4557.

[13] R. Gerald II, T. Bernhard, U. Haeberlen, J. Rendell, S. Opella, Chemical shift and electric field gradient tensors for the amide and carboxyl hydrogens in the model peptide N-acetyl-D,L-valine. Single-crystal deuterium NMR study, J. Am. Chem. Soc. 115 (1993) 777–782.

[14] Q.A. Wu, Z.Y. Xu, N-acetyl-L-valine, Acta Cryst., Sec. E 60 (2004) 949–950.

[15] R. Tycko, P.L. Stewart, S.J. Opella, Peptide plane orientations determined by fundamental and overtone nitrogen 14 NMR, J. Am. Chem. Soc. 108 (1986) 5419–5425.

[16] J.R. Brender, D.M. Taylor, A. Ramamoorthy, Orientation of amide–nitrogen-15 chemical shift tensors in peptides: a quantum chemical study, J. Am. Chem. Soc. 123 (2001) 914–922.

[17] M. Strohmeier, D. Stueber, D.M. Grant, Accurate ^{13}C and ^{15}N chemical shift and ^{14}N quadrupolar coupling constant calculations in amino acid crystals: Zwitterionic, hydrogen-bonded systems, J. Phys. A 107 (2003) 7629–7642.

[18] S. Hori, K. Yamauchi, S. Kuroki, Proton NMR chemical shift behavior of hydrogen-bonded amide proton of glycine-containing peptides and polypeptides as studied by *ab initio* mo calculation, Int. J. Mol. Sci. 3 (2002) 907–913.

[19] M. Torrent, D.G. Musaev, K. Morokuma, Calculation of nuclear quadrupole parameters in imidazole derivatives and extrapolation to coenzyme B$_{12}$. A theoretical study, J. Phys. Chem. B 103 (1999) 8618–8627.

[20] R. Ludwing, Structure of liquid *N*-methylacetamide: temperature dependence of NMR chemical shifts and quadrupole coupling constants, J. Phys. Chem. A 101 (1997) 8861–8870.

[21] F. Elmi, N.L. Hadipour, A study on the intermolecular hydrogen bonds of α-glycylglycine in its actual crystalline phase using ab initio calculated ^{14}N and ^{2}H nuclear quadrupole coupling constants, J. Phys. Chem. A 109 (2005) 1729–1733.

[22] N. Asakawa, S. Kuroki, H. Kurosu, I. Ando, A. Shoji, T. Ozaki, Hydrogen-bonding effect on carbon-13 NMR chemical shifts of L-alanine residue carbonyl carbons of peptides in the solid state, J. Am. Chem. Soc. 114 (1992) 3261–3265.

[23] M.J. Frisch, G.W. Trucks, H.B. Schlegel, G.E. Scuseria, M.A. Robb, J.R. Cheeseman, V.G. Zakrzewski, J.A. Montgomery Jr., R.E. Stratmann, J.C. Burant, S. Dapprich, J.M. Millam, A.D. Daniels, K.N. Kudin, M.C. Strain, O. Farkas, J. Tomasi, V. Barone, M. Cossi, R. Cammi, B. Mennucci, C. Pomelli, C. Adamo, S. Clifford, J. Ochterski, G.A. Petersson, P.Y. Ayala, Q. Cui, K. Morokuma, D.K. Malick, A.D. Rabuck, K. Raghavachari, J.B. Foresman, J. Cioslowski, J.V. Ortiz, A.G. Baboul, B.B. Stefanov, G. Liu, A. Liashenko, P. Piskorz, I. Komaromi, R. Gomperts, R.L. Martin, D.J. Fox, T. Keith, M.A. Al-Laham, C.Y. Peng, A. Nanayakkara, C. Gonzalez, M. Challacombe, P.M.W. Gill, B. Johnson, W. Chen, M.W. Wong, J.L. res, C. Gonzalez, M. Head-Gordon, E.S. Replogle, J.A. Pople, Gaussian 98, Gaussian Inc, Pittsburgh PA, 1998.

[24] T. Clark, J. Chrasekhar, G.W. Spitznagel, P.V.R. Schleyer, J. Comp. Chem. 294 (1983) 4.

[25] M. Mirzaei, N.L. Hadipour, An investigation of hydrogen-bonding effects on the nitrogen and hydrogen electric field gradient and chemical shielding tensors in the 9-methyladenine real crystalline structure: a density functional theory study, J. Phys. Chem. A 110 (2006) 4833–4838.

[26] H. Behzadi, N.L. Hadipour, M. Mirzaei, A density functional study of ^{17}O, ^{14}N and ^{2}H electric field gradient tensors in the real crystalline structure of α-glycine, Biophys. Chem. 125 (2007) 179–183.

[27] S.K. Amini, N.L. Hadipour, F. Elmi, A study of hydrogen bond of imidazole and its 4-nitro derivative by ab initio and DFT calculated NQR parameters, Chem. Phys. Lett. 391 (2004) 95–100.

[28] M.J. Duer, Solid State NMR Spectroscopy, Blackwell Science Ltd., London, 2002.

[29] G. Wu, S. Dong, R. Ida, N. Reen, A Solid-State ^{17}O Nuclear Magnetic Resonance Study of Nucleic Acid Bases, J. Am. Chem. Soc. 124 (2002) 1768–1777.

[30] R. Ida, M.D. Clerk, G. Wu, Influence of N–H···O and C–H···O hydrogen bonds on the ^{17}O NMR tensors in crystalline uracil: computational study, J. Phys. Chem. A 110 (2006) 1065–1071.

[31] G. Wu, S. Dong, R. Ida, Solid-state ^{17}O NMR of thymine: a potential new probe to nucleic acid base pairing, Chem. Commun. (2001) 891–892.

[32] J.K. Harper, G. McGeorge, D.M. Grant, Solid-state ^{13}C chemical shift tensors in terpenes. 2. NMR characterization of distinct molecules in the asymmetric unit and steric influences on shift in parthenolide, J. Am. Chem. Soc. 121 (1999) 6488–6496.

[33] J.C. Facelli, Density functional theory calculations of the structure and the ^{15}N and ^{13}C chemical shifts of methyl bacteriopheophorbide *a* and bacteriochlorophyll *a*, J. Phys. Chem. B 102 (1998) 2111–2116.

[34] A.D. Becke, Density-functional thermochemistry. III. The role of exact exchange, J. Chem. Phys. 98 (1993) 5648–5652.

[35] P. Pyykkö, Spectroscopic nuclear quadrupole moment, Mol. Phys. 99 (2001) 1617–1629.

[36] P.J. Carrol, P.L. Stewart, S. Opella, Structures of two model peptides: *N*-acetyl-D,L-valine and *N*-acetyl-L-valyl-L-leucine, J. Acta. Cryst., Sec. C 46 (1990) 243–246.

[37] A.B. Biswas, E.W. Hughes, B.D. Sharma, J.N. Wilson, The crystal structure of α-glycylglycine, Acta. Crystallogr. Sect. B 24 (1968) 40–50.

[38] R.E. Stark, R.A. Haberkorn, R.G. Graffin, ^{14}N NMR determination of NH bond lengths in solids, J. Chem. Phys. 68 (1978) 1996–1997.

[39] S. Ono, T. Taguma, S. Kuroki, I. Ando, H. Kimura, K. Yamauchi, A study of hydrogen-bonding of amino acids, peptides and polypeptides in the solid state as a function of temperature by static ^{2}H NMR method, J. Mol. Struct. 602-603 (2002) 49–58.

[40] M. Mirzaei, F. Elmi, N.L. Hadipour, A systematic investigation of hydrogen-bonding effects on the ^{17}O, ^{14}N, and ^{2}H nuclear quadrupole resonance parameters of anhydrous and monohydrated cytosine crystalline structures: a density functional theory study, J. Phys. Chem. B 110 (2006) 10991–10996.

[41] L.G. Butler, T.L. Brown, Nuclear quadrupole coupling constants and hydrogen bonding. Molecular orbital study of oxygen-17 and deuterium field gradients in formaldehyde-water hydrogen bonding, J. Am. Chem. Soc. 103 (1981) 6541–6549.

[42] S.J. Opella, P.L. Stewart, Methods Enzymol. 176 (1989) 242.

[43] H. Behzadi, M.D. Esrafili, N.L. Hadipour, A theoretical study of ^{17}O, ^{14}N and ^{2}H nuclear quadrupole coupling tensors in the real crystalline structure of acetaminophen, Chem. Phys. 333 (2007) 97–104.